X-chromosome-wide profiling of MSL-1 distribution and dosage compensation in *Drosophila*

Gaëlle Legube,[1] Shannon K. McWeeney,[2] Martin J. Lercher,[1,3] and Asifa Akhtar[1,4]

[1]European Molecular Biology Laboratory, 69117 Heidelberg, Germany; [2]Division of Biostatistics, Department of Public Health and Preventative Medicine, Oregon Health and Science University, Portland, Oregon 97239, USA; [3]Department of Biology and Biochemistry, University of Bath, Bath BA2 7AY, United Kingdom

In *Drosophila*, dosage compensation is achieved by a twofold up-regulation of the male X-linked genes and requires the association of the male-specific lethal complex (MSL) on the X chromosome. How the MSL complex is targeted to X-linked genes and whether its recruitment at a local level is necessary and sufficient to ensure dosage compensation remain poorly understood. Here we report the MSL-1-binding profile along the male X chromosome in embryos and male salivary glands isolated from third instar larvae using chromatin immunoprecipitation (ChIP) coupled with DNA microarray (ChIP–chip). This analysis has revealed that majority of the MSL-1 targets are primarily expressed during early embryogenesis and many target genes possess DNA replication element factor (DREF)-binding sites in their promoters. In addition, we show that MSL-1 distribution remains stable across development and that binding of MSL-1 on X-chromosomal genes does not correlate with transcription in male salivary glands. These results show that transcription per se on the X chromosome cannot be the sole signal for MSL-1 recruitment. Furthermore, genome-wide analysis of the dosage-compensated status of X-linked genes in male and female shows that most of the X chromosome remains compensated without direct MSL-1 binding near the gene. Our results, therefore, provide a comprehensive overview of MSL-1 binding and dosage-compensated status of X-linked genes and suggest a more global effect of MSL complex on X-chromosome regulation.

Dosage compensation ensures that, despite unequal numbers of X chromosomes, expression levels of X-linked genes are equal in males and females. During evolution, this process has evolved in different ways. In mammals, it is achieved by inactivation of one of the two female X chromosomes. In *Caenorhabditis elegans*, the two X chromosomes in hermaphrodites are repressed by a half. In contrast, in *Drosophila*, dosage compensation occurs by increasing transcription of most of the genes on the single male X chromosome (for review, see Baker et al. 1994). Genetics studies have led to the characterization of five genes, *male specific lethal-1*, *male specific lethal-2*, *male specific lethal-3*, *male absent on the first (mof)*, and *maleless (mle)*, all required for male viability. The products of these genes, as well as two noncoding RNAs (roX1 and roX2) assemble in a large complex, the dosage compensation complex (DCC), or MSL complex, which specifically targets hundreds of sites on the male X chromosome (Lucchesi et al. 2005; Straub et al. 2005a; Taipale and Akhtar 2005), together with the JIL1 protein, shown to be associated with the DCC (Jin et al. 2000).

Interestingly, this hyperactivation of the X-linked genes in males seems to be at least partially achieved at the level of chromatin. This is highlighted by the fact that at least two of the six proteins known to be involved in dosage compensation possess the ability to modify histones: MOF acetylates Lys 16 of histone H4 (Hilfiker et al. 1997; Akhtar and Becker 2000), while JIL1 phosophorylates Ser 10 of histone H3 (Wang et al. 2001). Both modifications have been previously linked to the regulation of transcription and chromatin structure (Turner 1998; Nowak and Corces 2004) and are significantly enriched on the male X chromosome in *Drosophila* (Bone et al. 1994; Jin et al. 2000).

One of the most intriguing aspects of dosage compensation is how this complex is able to target specifically hundreds of sites primarily on the X chromosome in order to ensure dosage compensation. Immunofluorescence studies on polytene chromosomes isolated from

[4]Corresponding author.
E-MAIL akhtar@embl.de; FAX 06221-387-518.

the salivary glands of male larvae have been used to study the targeting of the DCC on the X chromosome. According to these studies, the MSLs are distributed on hundreds of sites along the X chromosome, separated by gaps deprived of MSLs.

It has been proposed that the association of the MSL proteins on the X chromosome can be subdivided into two basic steps. The first step would include male-specific targeting of the MSL members to discrete sites on the chromosome (the "chromatin entry sites"), while the second step would involve the subsequent spreading of the complex, in a bidirectional but noncontinuous manner, to the flanking chromatin. This proposal came, first, from the observation that ~35–40 sites along the X chromosome can still retain MSL-1/MSL-2 in *msl3*, *mle*, and *mof* mutant backgrounds. Only two of these sites are fully characterized, and they correspond to the *roX1* and *roX2* genes. Importantly, they are able to attract the MSL complex when inserted on an autosome, leading to the theory of the "chromatin entry sites" (Lyman et al. 1997; Kelley et al. 1999). Second, the MSL complex, when targeted on an autosome by the insertion of a *roX1* transgene, has the ability to spread over the surrounding chromatin (Kelley et al. 1999). However, this model appears now to be too simple. Indeed, any piece of the X chromosome is able to attract the complex when moved onto an autosome, even without any of the 35–40 "entry sites" (Oh et al. 2003; Fagegaltier and Baker 2004). Another model to explain MSL targeting has emerged from a recent study, which showed that recruitment of the MSLs can be induced by transcription activation of a transgene inserted in a band normally deprived in MSL (Sass et al. 2003). In addition, the distribution of the MSL complex on the X in ovaries is distinct from the distribution reported for salivary gland polytene squashes (Sass et al. 2003), indicating that the DCC distribution could reflect cell type expression patterns. These data suggested that transcription activation on the X chromosome by itself could act as a signal to recruit the DCC.

Another intriguing and poorly understood aspect of this process is how the twofold up-regulation of X-linked genes is achieved. MSL recruitment appears to be causal for transcriptional activation. Indeed, MOF is able to relieve chromatin-mediated repression of transcription in vitro and in vivo when targeted to a promoter (Akhtar and Becker 2000). Moreover, targeting the DCC artificially on an autosome leads to up-regulation of the downstream gene (Henry et al. 2001; Park et al. 2002). However, the transcriptional activation performed by the MSL complex should not overcome individual gene regulation, linked to developmental pathways, but rather fine-tune the transcription to ensure dosage compensation. How this twofold fine-tuning of transcription is achieved remains unclear. More specifically, whether the recruitment of the MSLs on X-linked genes at a local level is both necessary and sufficient to ensure a twofold overactivation of the target gene is still unknown. Apart from *roX* genes, only a few other X-linked genes have been shown to be targeted by the MSL complex. Chromatin immunoprecipitation (ChIP) studies have shown

that the DCC is enriched on the *zw* gene, known to be dosage-compensated, and is not present on the *runt* gene, compensated by an MSL-independent process (Smith et al. 2001). However, some genes, such as *lsp1α*, have been reported to not be compensated at all, although they are located in bands highly enriched in DCC as assessed by immunofluorescence. Conversely, the *sgs4* gene, compensated in a DCC-dependent manner (Chiang and Kurnit 2003), is located on the 3C10 cytological band, which is depleted in MSL proteins (Demakova et al. 2003).

ChIP followed by microarray (ChIP–chip) has been performed in a diverse array of taxa and has provided a comprehensive view of the distribution of a variety of transcription factors, coactivators, corepressors, or histone modifications (van Steensel 2005). These genome-wide analyses have been shown to be particularly powerful in correlating the structure of chromatin with its functional state, and in understanding modes of targeting of different factors. Given the exciting potential of these techniques with respect to the targeting of the MSL complex and the dosage compensation mechanism, we decided to utilize it to analyze the distribution of MSL-1 along the X chromosome, and to compare this with expression levels in males and females. To test whether MSL-1 distribution reflects cell type or developmental expression pattern, we have mapped the distribution of MSL-1 in overnight embryos, as well as in 4–6-h early embryos and in salivary glands from larvae. We also analyzed expression profiles in salivary glands from male and female third instar larvae using microarrays, to study the correlation between the presence of the complex, the transcriptional state, and the "dosage-compensated" state of X-linked genes.

Results

Mapping of the DCC distribution in embryos

In order to map the in vivo target genes of the DCC, we first performed ChIP–chip analysis from 0–14-h wild-type embryos with specific antibodies against MSL-1. The DNA amplified from the MSL-1 immunoprecipitation was labeled with Cy5 fluorophore and hybridized against DNA amplified from a nonspecific immunoprecipitation (mock IP), labeled with Cy3 dye. We used a cDNA array covering the DGC1 and DGC2 cDNA libraries from the Berkeley *Drosophila* Genome Project (see Materials and Methods), which represents >70% of the coding sequences of the *Drosophila* genome (Stapleton et al. 2002). Of the 10,188 spotted clones that have chromosomal annotation, 1699 (i.e., 16.6%) are located on the X chromosome, representing 73.6% of the annotated features on the X (based on Flybase version 4.2.1 annotation). All raw data are publicly available on Array Express (http://www.ebi.ac.uk/arrayexpress/query/entry, accession no. E-MEXP-554). For comparative analysis MSL-3 IP was performed in parallel (Supplementary Table 1).

The *roX1* gene has previously shown to be enriched for the MSL proteins in many systems (embryos, third instar larvae salivary glands, SL-2 cells) (Smith et al. 2001) and,

therefore, can serve as an internal positive control for the arrays. Consistent with previous observations we also found that *roX1* was significantly enriched for both MSL-1 and MSL-3 ($p = 0.00025$ for MSL-1, $p = 0.01556$ for MSL-3) in our arrays. The *runt* gene, previously reported to be depleted of MSL complex, was used as a negative internal control and was not significant for either MSL-1 ($p = 0.68$) or MSL-3 ($p = 0.82$). In addition, we performed quantitative PCR (qPCR) on 20 clones for further validation. There was a significant correlation between the enrichment ratios (MSL-1/mock) obtained by qPCR and the microarray ($r = 0.77$, p-value $< 10^{-4}$) (Supplementary Fig. 1).

To identify the candidate MSL-1 target population, we used the joint criteria of statistical significance and rank (p-value < 0.1 and median percentile rank across the arrays >95%) (Supplementary Table 2). After removal of the clones that do not have chromosomal annotation, 82% of the clones identified by these joint criteria (96 out of 117) were located on the X chromosome, in agreement with immunofluorescence studies on polytenes chromosomes (Fig. 1A). It is interesting to note that the MSL complex has been reported to interact also with a few sites on autosomes (Demakova et al. 2003), which could explain the presence of autosomal genes in the MSL-1 target clone subset.

A sample ($n = 7$) of clones from the candidate target list on the X was selected for further validation. There was 100% confirmation of MSL-1 enrichment by qPCR (Supplementary Fig. 1). In addition, four clones located on the X chromosome that did not meet the candidate target criteria were also examined by qPCR. No significant enrichment over the mock IP was seen for these clones (Supplementary Fig. 1).
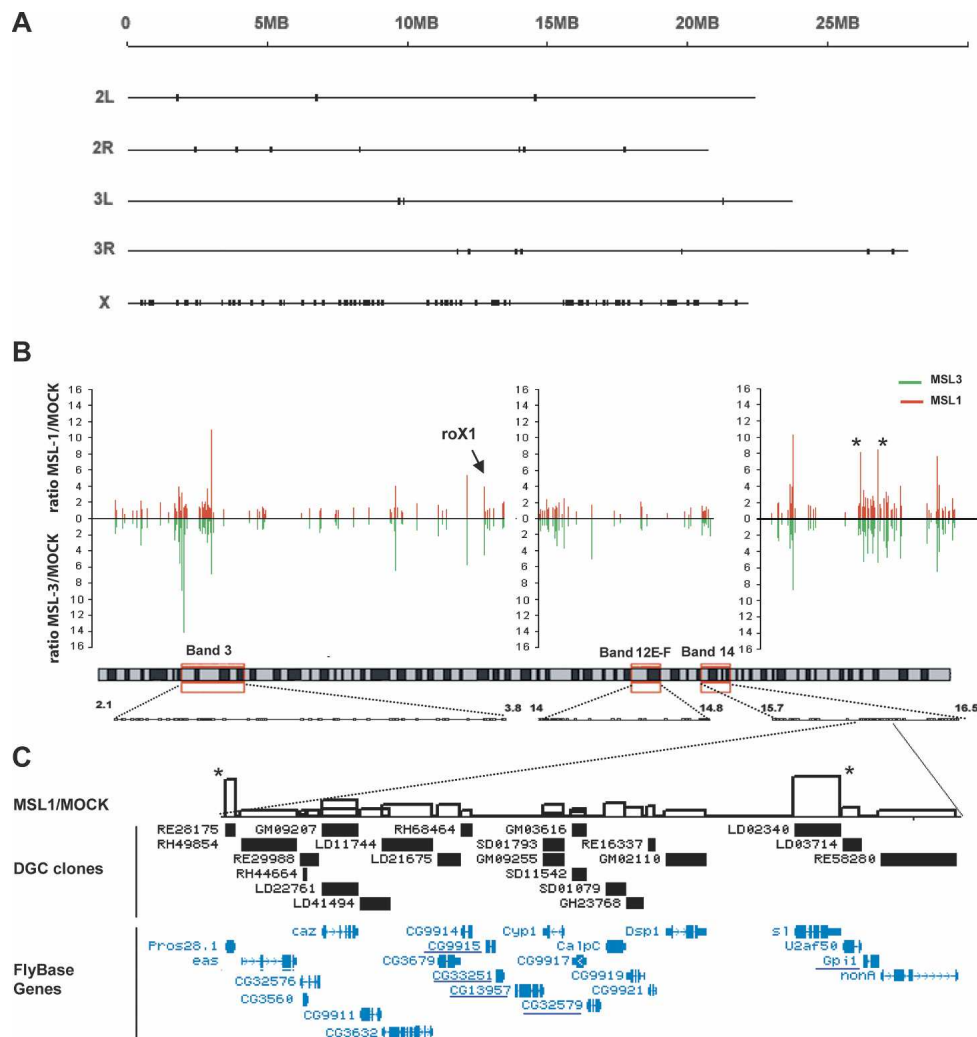
Figure 1. Binding of MSL-1 and MSL-3 in 0–14-h *Drosophila* embryos. (*A*) Chromosomal distribution of MSL-1 target genes in 0–14-h embryos, defined as the genes showing a rank percentile > 95%, and a *p*-value < 0.1. The majority of these genes are located on the X chromosome as shown. (*B*) Distribution of MSL-1 (in red) and MSL-3 (in green) on three cytological bands of the X chromosome. Each vertical line represents the average MSL-1/MOCK ratio of a probed gene at its chromosomal position (in megabases). Positions of the DGC clones spotted on the array are presented *below* each graph. The *roX1* gene is indicated by an arrow. Asterisk indicates cluster of genes represented in *C*. (*C*) Detailed view of a cluster of genes located in the 14 cytological band.

The distribution of MSL-1 and MSL-3 binding across the X was examined (using gene positions from the Berkeley *Drosophila* Genome Project release 4.1) (Fig. 1B). As expected, the distribution of MSL-1 (represented in Fig. 1B, in red) overlapped with that of MSL-3 (represented in green) (with 34 [or 42%] of the MSL-3 targets seen in MSL-1). There was a strong correlation between the binding of MSL-1 and of MSL-3 (values expressed as log ratios) on the X ($r = 0.81$, $p < 10^{-4}$) (Supplementary Fig. 2). Finally, X-linked genes identified by our criteria as candidate targets with MSL-1 had a median percentile rank of 94% for MSL-3, indicative of a high concordance between the target gene populations for MSL-1 and MSL-3 (Supplementary Table 2). Taken together, these results indicate that MSL-1 and MSL-3 bind highly overlapping target sites across the X chromosome in embryos.

Interestingly, MSL-1 and MSL-3 appear to be targeted at the individual gene level, reflected in the varied level of MSL complex enrichment within clusters of genes (e.g., the clusters of genes on cytological bands 3 and 14 in Fig. 1B). It is of course possible that MSL-1/3 may also bind to intergenic or intronic regions, or to additional genes missing from our arrays. However, a close-up of 95 kb of a gene dense region well tiled on our array (18 out of the 23 genes represented, covering ~66 kb) confirmed this finding (Fig. 1C). For example we observed enrichment of MSL-1 on the *sl* gene, whereas *U2af50* shows a background enrichment level, although located <0.5 kb from *sl*. This wide variability of MSL-1 targeting among neighboring loci shows for the first time that the complex targets discrete loci and not broad chromosome domains. In addition, these results indicate that our ChIP data provide sufficient resolution to allow further analysis of the target gene population.

Functional features of MSL-1 target genes: MSL-1 binds genes with shared expression profile and transcription factor motifs

In order to better understand the modes of MSL targeting, we decided to investigate the different functional characteristics of these X-linked genes highly enriched in MSL-1. For comparative purposes, we defined a category of X-linked "nontarget" genes (*p*-value > 0.6 and percentile rank < 60% for both MSL-1 and MSL-3 data). First, considering that without dosage compensation males die, we wondered whether these target genes are essential for life. For this analysis we used the data generated by the large-scale P-element insertion screens (Bourbon et al. 2002; Peter et al. 2002). There was no significant association between the phenotype (lethal or not) and the target status (data not shown), even though we could observe a slight preference of MSL-1 targeting on essential genes, as 12.5% of the MSL-1 targeted genes were essential whereas this was the case for only 7% of the nontargeted genes.

We next addressed whether targeting of the MSL-1 happens on genes sharing common transcription factor-binding sites. For this purpose we used the REDUCE

algorithm (http://bussemaker.bio.columbia.edu:8080/reduce) that has been designed for the discovery of regulatory elements based on microarray expression data, in an unbiased manner (Bussemaker et al. 2001). We performed REDUCE analysis on the 1-kb upstream sequences of the entire set of probed loci to discover motifs that correlate with the chromatin profiling data for MSL-1. We found an overrepresentation of motifs that are part of the DNA replication-related element (DRE), targeted by DREF (DNA replication element factor), among the most significant motifs. We further confirmed this result by comparing the target and nontarget populations for the presence of DRE elements; 28.2% of the target gene indeed possessed at least one consensus DRE site in their 3-kb upstream sequence, versus only 15.8% for the nontarget genes (Fisher exact $p = 0.0034$).

Finally, we asked whether the MSL-1 target genes share similar expression patterns during development. For this analysis we used the Yale *Drosophila* developmental transcriptional time course data set (Arbeitman et al. 2002). In addition to differential gene expression analysis, cluster analysis (average linkage using a correlation metric) was performed to aid in visualization (Cluster and Treeview software programs, http://rana.lbl.gov/EisenSoftware.htm). Strikingly, most of the MSL-1 target genes for which expression data are available exhibited differential expression levels between early embryogenesis and later developmental stages, which was not observed for the nontarget population (Fig. 2). Most of them showed higher expression level until 11–12 h after fertilization (with an average log ratio of 0.46 for the target against –0.019 for the nontarget). Even when using the most stringent post-hoc multiple comparison adjustment (Bonferroni), these differences in expression were significant between target and nontarget populations at each of the seven early embryonic time points in the Arbeitman data set (up to 25 h, all adjusted *p*-values < 0.05).

Taken together, these data show that, in embryos, MSL-1 is targeted on genes sharing common functional features such as common DREF-binding sites and similar expression patterns during development.

The distribution of the MSL-1 is stable between early embryos and salivary glands of third instar larvae

The above results also suggest that targeting of MSL-1 may correlate with transcription activation, as we observe MSL-1 binding in 0–14-h embryos, on genes that are highly transcribed during early embryogenesis. Recent data have indeed led to the proposal that the MSL-binding pattern on the X chromosome could reflect the cell-type-specific gene expression patterns (Sass et al. 2003). In order to investigate this point in detail we decided to study whether the localization of MSL-1 changes during development. For this purpose we compared the distribution of MSL-1 at two different developmental stages. Chromatin was prepared from tightly staged early embryos (4–6 h), where dosage compensation is just established (Rastelli et al. 1995; Franke et al.
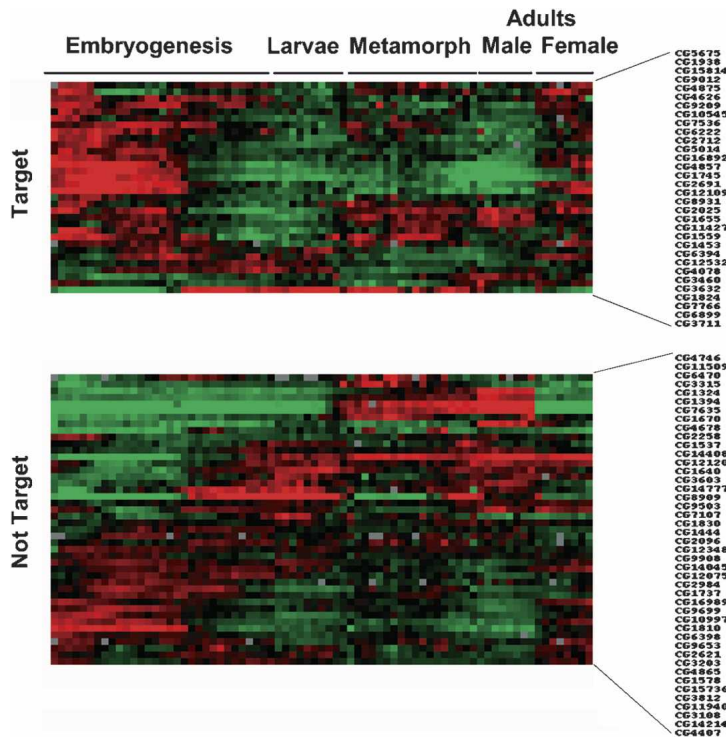
Figure 2. MSL-1 binds on active genes early in development. Clustered expression profiles of target and nontarget genes of MSL-1 in 0–14-h embryos. Most target genes are predominantly expressed in embryos. Red indicates high expression level, green indicates low expression level. Gene expression data were taken from Arbeitman et al. (2002).

1996) and from dissected male salivary glands isolated from third instar larvae. This strategy ensured chromatin preparation and further analysis on a more homogenous population. Furthermore, analyzing the distribution pattern of MSL-1 in salivary glands also allowed us to compare the results with pre-existing data of MSL-1 localization from immunofluorescence studies on polytene chromosomes.

As expected, *roX1* showed a strong enrichment level in both data sets (larvae: $p = 0.093$, rank = 99.2%; 4–6-h embryos: $p = 0.0119$, rank = 98.8%). We used the same criteria as previously to define the subset of target genes ($p < 0.1$, rank percentile > 95%). For salivary glands and 4–6-h embryos, 86% and 89% of the clones following these criteria were located on the X chromosome, respectively (i.e., 197/229 and 407/457 that possess chromosomal annotation, respectively; Supplementary Table 2). The cytological region 12E6–12F3 previously reported to be depleted of MSL proteins on polytene squashes (Demakova et al. 2003) appeared depleted of MSL-1 also in our salivary glands ChIP–chip analysis, further validating the results (Fig. 3A).

Interestingly, MSL-1 targeting in 4–6-h embryos is correlated with MSL-1 targeting in larvae on the X chromosome ($r = 0.69$, $p < 10^{-4}$) (Fig. 3B). Among the 407 clones target in 4–6-h embryos, 40% (i.e., 163) were still able to attract the complex in larvae, representing 82.7% of the larvae target population. This strong overlap seen between the two populations of target genes indicated that most of the genes targeted by MSL-1 in larvae appear to have already been targets in 4–6-h embryos.

Taken together, these results indicate that the pattern of MSL-1 binding is set up early in development, with MSL-1 binding in later stages presenting a subset of binding in earlier stages. This might also explain why we could identify many more MSL-1-binding sites in 4–6-h embryos compared with overnight embryos and larvae, although this difference could also be related to different efficiencies of immunoprecipitation.

Correlation between MSL-1 targeting and transcription

The above results argue against a correlation between transcription and targeting since many genes expressed during embryogenesis undergo inactivation during larval stages (Arbeitman et al. 2002), whereas MSL-1 appears stably bound on the X chromosome across development. We, therefore, further investigated the relationship between transcription activation and MSL-1 targeting.

First, we compared our ChIP–chip data with the expression data available on the Yale *Drosophila* lifetime course (Arbeitman et al. 2002). The scatter plots presented in Figure 4A show the correlation between targeting (log ratio MSL-1/MOCK) and the transcription (log ratio time point/pool) for all the DGC clones on the X chromosome. We found a weak correlation between transcription and MSL-1 binding in 4–6-h embryos (ranging from $r = 0.29$–0.33 depending on the time point considered [4–5 h or 5–6 h], $p < 10^{-4}$), but surprisingly we did not find any biologically significant correlation when we compared our ChIP–chip results in third instar larvae salivary glands with the 96-h or 105-h expression time points (respectively, $r = -0.09$, $p = 0.04$; $r = -0.04$, $p = 0.3$) (Fig. 4A, left and middle panels). However, the differences could be due to the fact that previous expression profiles were generated using whole larvae (Arbeitman et
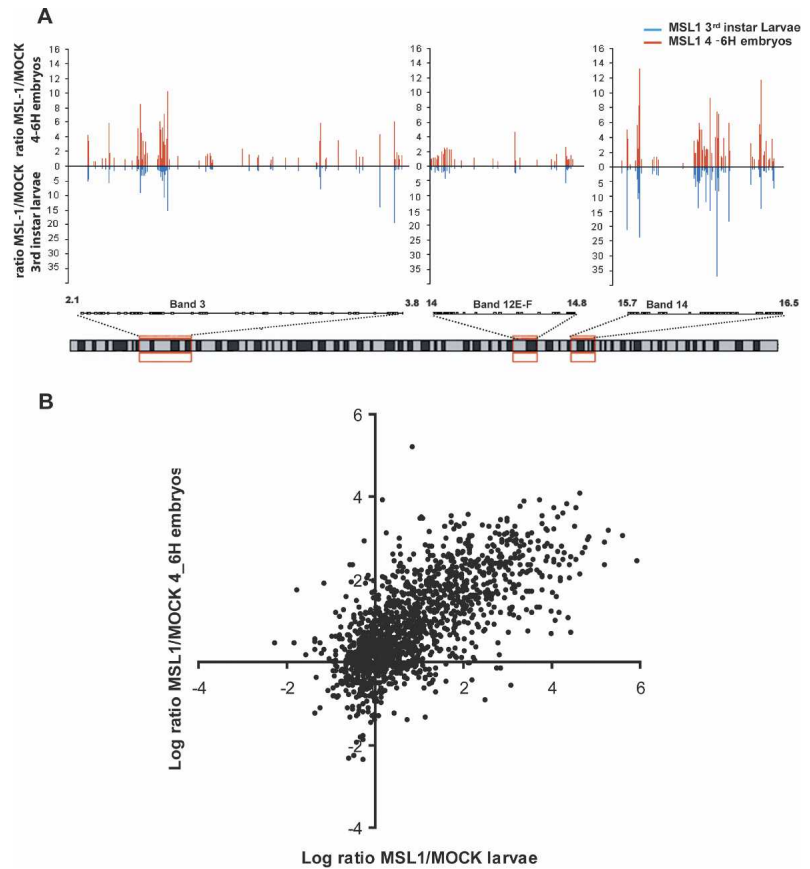
Figure 3. Similar distribution of MSL-1 binding between 4–6-h embryos and salivary glands of third instar larvae. (*A*) Distribution of MSL-1 in 4–6-h-staged embryos (in red) and in male third instar larvae salivary glands (in blue) on the same three cytological bands of the X chromosome represented in Figure 1B. (*B*) Bivariate scatterplot of MSL-1/MOCK log ratio in 4–6-h embryos and in third instar larvae salivary glands of all probed loci on the X chromosome.

al. 2002), while our ChIP analysis is performed on isolated salivary glands. Therefore, in order to investigate more rigorously whether MSL-1 targeting correlates with transcription activation of X-linked genes, the MSL-1 localization was compared with the transcription profile in salivary glands. For this purpose, we purified RNA from male third instar larvae salivary glands, and hybridized it against a pool of RNA on the same DGC-microarray in order to directly compare the MSL-1-binding profile with the expression profile of the X-linked genes.

Of the X-linked clones spotted on the array, 1035 clones exhibited a signal for the pool RNA above background, defining a category suitable for further analysis. In agreement with the correlation obtained using the whole larvae time point expression data, the correlation between MSL-1 binding and transcription in salivary glands was very weak ($r = 0.10$, $p < 0.001$) (Fig. 4A, right panel). This was further confirmed by comparing the distribution of expression levels between the target genes and the nontarget gene subset. The RNA levels (expressed as the log ratio male salivary glands/pool) of the targeted genes were not significantly different from the one of not targeted genes in male third instar larvae salivary glands (data not shown).

Rather than looking at the entire data set as performed above, we then defined subsets of genes as "expressed" or "not expressed." Of the 1035 X-linked clones previously selected, 884 showed an RNA level in salivary glands above background threshold levels (based on negative controls) defining our class of expressed genes, whereas 151 did not, thus representing a not expressed class of genes. The MSL-1 targeting status of genes in both sets (expressed and nonexpressed) was examined. We observed a significant association between targeting and transcription (Fisher's exact $p = 0.023$) with a preference for the target genes to be transcribed. However, 13 out of the 149 MSL-1 target clones were not expressed (i.e., 8.7%), indicating that targeting of the MSL-1 by itself does not induce transcription activation, at least not to a level we could detect in our experiments.

It was surprising that only 136 of the 884 expressed genes (i.e., 15.4%) were bound by MSL-1, indicating that expression of X-linked genes does often not lead to MSL-1 binding. Since we cannot rule out that we may have missed some target sites due to the stringency of our criteria as well as the nature of the cDNA arrays, it remains to be seen what proportion of the remaining expressed genes may be targeted by MSL-1.

We also performed immunostaining of polytene chromosomes isolated from salivary glands of third instar larvae, using MSL-1 antibody in combination with Spt5, Spt6 (elongation factors), or PolII-S5-P antibody (active form of the RNA polymerase II). Strikingly, this analysis, even though allowing a lower resolution than the ChIP–chip, also showed a distinct binding pattern of MSL-1

A

B
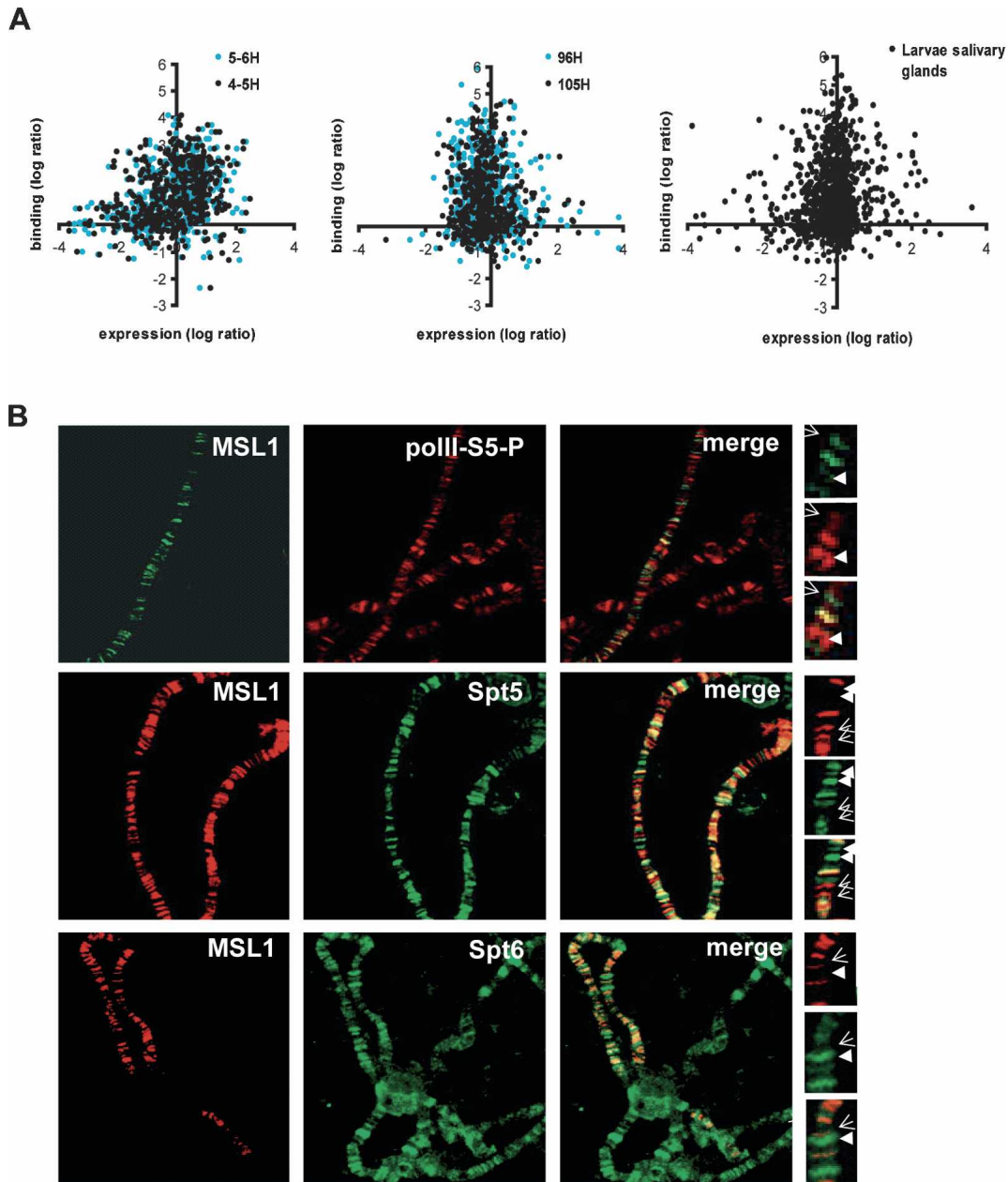
Figure 4. MSL-1 binding correlates poorly with transcription in male salivary glands. (*A*) Bivariate scatterplots of MSL-1/MOCK ChIP data and time point/pool expression data. MSL-1/MOCK log ratio is obtained from the 4–6-h ChIP–chip data set (*left* panel) and from the male third instar salivary glands ChIP–chip data set (*middle* and *right* panels). Time point/pool log ratio are obtained from the 4–5-h (in black) and 5–6-h (in blue) time points (*left* panel); from the 96-h (in blue) and 105-h (in black) time points (*middle* panel) (Arbeitman et al. 2002); and from the male salivary gland expression data set (analyzed from four independent experiments, our results) (*right* panel). (*B*) Immunofluorescence analysis of the distribution of MSL-1 and of three transcription-associated factors on male polytene chromosomes from third instar larvae Spt5, Spt6, and RNA polymerase II (PolII-S5-P; phosphorylated on the Ser 5 of the CTD).

and other transcription-associated factors in salivary glands. Spt6, Spt5, or PolII-S5-P could immunostain bands depleted in MSL-1, and vice versa (Fig. 4B), further supporting the array data.

Taken together, these results show that even though MSL-1 preferentially binds active genes, transcription per se is not sufficient or required for MSL-1 localization on the X chromosome.

Correlation between dosage compensation and MSL-1 binding

Next we were interested to study the dosage compensation status of the X-linked genes that are bound or not bound by MSL-1, since we found high proportion of transcribed genes not bound by MSL-1. For this purpose we purified RNA from female salivary glands and hybridized

it, against the same pool of RNA as previously used for male expression profile analysis.

The expression data obtained for female are highly similar to that seen in male (Fig. 5A) ($r = 0.94$, $p < 10^{-4}$), suggesting that most genes are compensated on the X chromosome, at least in salivary glands of third instar larvae. Since studying twofold expression level differences is difficult in an array experiment, we imposed stringent criteria to define a "dosage-compensated" subset (FDR adjust $p = 1$) to ensure further analysis on a more strict population, even if it was at the expense of missing a fraction of dosage-compensated genes. Using these criteria we found that 588 out of the 884 transcribed genes are compensated, representing ~66.4% of the transcribed genes.

When we compared target and dosage compensation status we found that there was no difference in the distributions, with 72% of the target and 68% of the nontarget populations considered to be dosage-compensated. Even though there is a slight tendency for the target

population to be dosage-compensated, these results indicate that there is no clear relationship between dosage-compensation and MSL-1 target status in salivary glands.

Since we were concerned that, even after using restrictive criteria based on FDR-adjusted p-values, we may still overrepresent the dosage-compensated population, we performed qPCR on a set of X-linked genes, showing different MSL-1 enrichment status. Among the 16 genes we tested, all the genes showing an FDR adjust $p = 1$ in our array experiment (Fig. 5B, in blue) also appeared compensated by qPCR analysis, validating the criteria we applied previously to define our dosage-compensated subset. In addition, genes that showed a low FDR p-value ($p < 0.1$) together with female-biased expression (in red) also appeared to be not compensated by qPCR. *BR-C* represents an example of the genes that we missed by applying stringent criteria (FDR $p = 1$) to define the dosage-compensated population. Indeed, although this gene has been excluded from our dosage-compensated subset
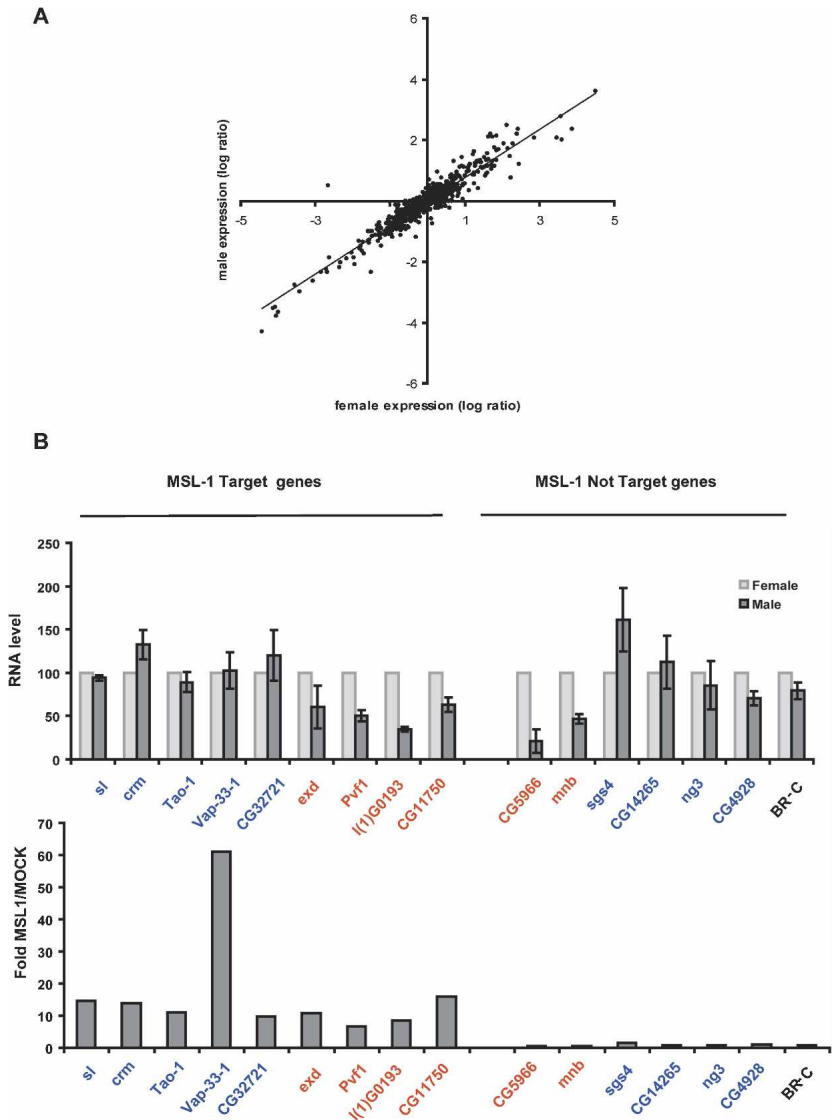
Figure 5. Direct MSL-1 binding is uncoupled at a local level with dosage compensation. (*A*) Bivariate scatter plot of the expression data (expressed as log ratio) obtained from male and female salivary glands, for the clones located on the X chromosome. (*B, top*) qPCR analysis of the RNA level in third instar salivary glands, in male and female, of nine genes "targeted" by MSL-1 according to our ChIP–chip analysis in larvae ($p < 0.1$, rank percentile > 95%), and seven genes defined as "not targeted" in salivary glands ($p > 0.6$, rank percentile < 60%). The genes that were part of the dosage-compensated subset according to the expression array data are shown in blue (FDR $p = 1$), whereas the genes in red showed an adjusted FDR p-value < 0.1; i.e., female-biased expression. All RNA levels were normalized against GAPDH. Male RNA levels are expressed as percentage of female expression level set at 100%. (*Bottom*) Binding profile of MSL-1 on the corresponding genes in the *top* panel represented by fold enrichment of MSL-1/MOCK in ChIP–chip salivary glands data set.

since it showed an FDR $p = 0.96$, it appeared compensated by qPCR analysis.

As observed using our microarray data, the enrichment status did not always correlate with the dosage-compensated state. Among the nine genes of the target subset that we tested in qPCR, five (*sl*, *crm*, *tao-1*, *vap-33-1*, and *CG32721*) were either expressed at equal level in male and female (i.e., dosage-compensated), or slightly higher in male than in female. However, four genes (*exd*, *pvf1*, *l(1)G0193*, and *CG11750*) did not appear to be dosage-compensated since they showed twofold lower expression in male than in female (Fig. 5B, genes "target"), indicating that some genes can escape dosage compensation, even though they are bound by the MSL complex.

Among the seven genes scored as MSL-1 "not target" ($p > 0.6$ and rank percentile < 60%) that we tested by qPCR, 2 (*mnb* and *CG5966*) showed lower expression in males compared with females. However, five genes (*sgs4*, *CG14265*, *ng3*, *CG4928*, *BR-C*) showed similar expression between male and female (i.e., dosage-compensated), or a tendency to be higher expressed in male. Taken together, these data show that both MSL-1-bound and unbound populations are comprised of dosage-compensated and nondosage-compensated genes.

Discussion

In this study we report genome-wide profile of MSL-1 distribution along the X chromosome in embryos and salivary glands isolated from third instar larvae. Our results show that most MSL-1-bound genes are expressed early in embryogenesis. The MSL-1 distribution appears to be set up early in development. Intriguingly, we find that even though most of the MSL-1 target genes are transcribed, target genes account for only a subset of transcribed genes on the X chromosome. This indicates that binding of MSL-1 on an X-linked gene is not a prerequisite for transcription activation in larvae, and that transcription on the X by itself cannot be the sole signal to attract the DCC. Furthermore, we found that a high proportion of both MSL-1 target and nontarget genes appears dosage-compensated, suggesting a global role of the MSL complex in X-chromosomal regulation.

Targeting of the MSL complex on the X chromosome

Using the ChIP–chip strategy, we examined the MSL-1 distribution on the *Drosophila* genome in order to investigate how the MSL complex achieves specific targeting on the X chromosome. Our analysis provides a first comprehensive list of MSL-1-binding sites along the X chromosome in early embryos and male salivary glands. Furthermore, we show that MSL-1 binds individual gene loci rather than broad chromosomal domains, which could not be addressed previously (Straub et al. 2005b).

More specifically, we wanted to address whether or not binding of MSL-1 is directed by transcription activation, since it was recently shown that driving transcription from a transgene inserted on the X chromosome is able to induce local DCC recruitment (Sass et al. 2003). Our results show that even though the MSL complex is predominantly bound on transcriptionally active genes, transcription of endogenous X-linked genes per se is not sufficient to attract the complex in salivary glands. This conclusion is based on the following observations. The first evidence is provided by the fact that the MSL-1 distribution is highly stable between two tissues as different as whole 4–6-h embryos and third instar salivary glands, indicating that the MSL distribution is unlikely to reflect expression profiles. Indeed, 40% of the target genes in 4–6-h embryos were still bound by MSL-1 in larvae, which represent most (82.7%) of the MSL-1 target genes in salivary glands. Furthermore by comparing expression and MSL-1-binding profiles in male salivary glands, we observe that recruitment of the MSL complex is not a general property of active X-linked genes, since only 15% of transcribed genes present on our array are directly bound by MSL-1. It remains possible that we may have missed a number of target sites in the intergenic or intronic regions since our analysis was performed on cDNA arrays. However, the comparison of the MSL-1-binding pattern with transcription-associated factors such as Spt-5, Spt-6, and S5-P PolII on intact polytene chromosomes also did not reveal a strong overlap between these proteins and MSL-1. These results are also consistent with recent observations (Kotlikova et al. 2006) that these transcription-associated factors localize both in bands enriched in MSL-1 and in bands depleted of MSL-1.

How is then the MSL complex targeted on the X chromosome? It is possible that transcription on the X acts as a signal for MSL-1 targeting during early stages of development. Once bound, the complex would then either be stabilized on the target genes or decay, independently of further changes in expression (accounting for the absence of major developmental change in the DCC distribution). In favor for this model we observed that MSL-1 binding correlates more with transcription in early embryos ($r = 0.3$) than in larvae ($r = 0.1$) (Fig. 4A), and that most of the MSL-1 target genes in all the stages we tested show high expression levels during early embryogenesis (Fig. 2; data not shown).

Alternatively, MSL-1 could be targeted by specific transcription factors to a small subset of genes. Indeed we observed that MSL-1 target genes are enriched in DREF-binding sites. DREF had previously been identified as a potential regulator of genes involved in cell cycle and growth regulation. DREF associates in vivo with the core promoter transcription complex TRF2 (TBP-related factor 2) and it has been proposed that it may target TRF2 to a subset of core promoters (Hochheimer et al. 2002). In a similar way DREF may promote gene selectivity for the DCC and act as a DNA-targeting component for the DCC. Consistent with this hypothesis, we found that the X chromosome is enriched in comparison to autosomes in genes that possess several DRE or DRE-related sites in their 2-kb upstream sequence (data not shown). Another interesting candidate would be the GAGA factor (GAF), which has been shown

to colocalize to some extent with the MSL complex on polytene chromosomes, and which is required for the proper localization of MSL on the X chromosome (Greenberg et al. 2004). It is noteworthy that the transgenes that were previously shown to attract the MSL complex when transcribed also possessed a few GAF-binding sites (Sass et al. 2003). A careful analysis of our MSL-1 distribution in 0–14-h embryos revealed that MSL-1 target genes are slightly more enriched in GAF-binding sites than nontarget genes (G. Legube, S.K. McWeeney, and A. Akhtar, unpubl.).

Targeting of MSL proteins on selected X-linked genes could then be achieved by a combinatorial effect of several independent motifs. This may explain why previous attempts to find specific X-chromosomal consensus sequences were not successful. Therefore, ChIP–chip approaches such as used in this study, which allow the discovery of physiological targets in an unbiased and global manner, will be important to unravel the complexity hidden within this system.

Role of the MSL complex in transcription activation and dosage compensation

In addition to providing insights into the MSL-1 targeting mechanism, our data also raise important questions about the role of the MSL complex in transcription activation and in the dosage compensation mechanism. First of all, according to our data, >66% of the transcribed X-linked genes are compensated, whereas only 15% are bound by MSL-1. Moreover, our array and qPCR analyses suggest that local MSL-1 binding is neither sufficient nor necessary to ensure dosage compensation in salivary glands.

One possibility is that the genes not bound by the MSL complex, but still compensated, could be up-regulated by an MSL-independent mechanism. However, we consider this possibility unlikely, as such an MSL-independent mechanism would have been already discovered by genetic screens (since it would then concern most of the dosage-compensated genes). In addition most of the genes on the X chromosome seem to be compensated in an MSL-2-dependent manner (Hamada et al. 2005). Therefore, we favor the idea that the MSL complex could have long-range effects on the transcription of X-linked genes. It has been already reported that the *Sgs4* and *BR-C* genes are dosage-compensated in third instar larvae in an MSL-dependent manner (Chiang and Kurnit 2003). Both of them are not bound by MSL-1 according to our data, and moreover *Sgs4* is localized in a band depleted in MSLs as assessed by immunofluorescence on polytene chromosomes (Demakova et al. 2003), supporting the idea of an action of MSL in a long-range manner.

How the MSL complex could operate to fine-tune the transcription of genes, distant from the direct MSL-binding sites, still remains a mystery. One exciting possibility may be that the MSL complex is actually required to recruit parts of the X chromosome into a nuclear domain with unique transcriptional/post-transcriptional proper-

ties. It has become clear that spatial positioning within the nucleus also plays a central role in the control of gene expression, allowing the coregulation of subsets of genes (Schubeler et al. 2000; Ragoczy et al. 2003; Chambeyron and Bickmore 2004). MSL binding on discrete loci could induce the localization of a broad X-chromosomal domain, containing several genes, to a nuclear compartment that possesses specific transcriptional properties. This may ensure the dosage compensation of many X-linked genes, without a need of direct MSL binding on these genes. Interestingly, purification of the MSL complex has revealed coassociation of several nucleoporins in embryos and Schneider cells (Mendjan et al. 2006). One may envisage that concerted action of MSL with nuclear pore components may help to define such domains needed for *cis*-regulation of many genes.

An interesting feature of the dosage-compensated X-chromosome includes the colocalization of MSL proteins with specific histone H4 Lys 16 acetylation (H4-K16Ac). This histone modification has been proposed many times to be related to transcription activation and appears to have a unique, although still poorly understood, role in transcriptional regulation (Dion et al. 2005). In *Drosophila*, H4-K16 acetylation overlaps with MSL binding on the male X chromosome on polytene chromosomes (Turner et al. 1992), and driving artificially H4-K16 acetylation by MOF is able to increase transcription (Akhtar and Becker 2000). However, the situation for endogenous X-linked genes appears to be more complex, at least in salivary glands, since we were able to find a number of genes bound by MSL-1 that did not seem to be transcribed (Fig. 4B). Interestingly, and in agreement with our observation in *Drosophila*, genome-wide analysis in *Saccharomyces cerevisae* showed that the distribution of H4-K16 acetylation along the chromosomes does not correlate with transcriptional activity (Kurdistani et al. 2004). Therefore, the function of H4-K16 acetylation in the dosage compensation process and more generally in transcriptional regulation appears unclear.

Another important issue to consider is that *Drosophila* salivary glands, although differentiated, undergo endoreplication (for review, see Edgar and Orr-Weaver 2001). Global analyses revealed that there is a correlation between replication timing and transcription activity. However, this correlation is not absolute (Schubeler et al. 2002; MacAlpine et al. 2004; Belyakin et al. 2005). Furthermore, similar replication timing profiles were obtained in two human cell types as different as fibroblasts and lymphoblasts, expected to show quite different gene expression profiles (White et al. 2004). Since H4 hyperacetylation has been associated with active replication origins (Aggarwal and Calvi 2004), it is tempting to speculate that MSL/H4-K16Ac distributions may correlate with replication timing. Interestingly, the DREF transcription factor, which binds the DRE sequence, identified in our MSL-1 target genes, plays a role in endoreplication in salivary glands (Hirose et al. 1999). Future global analyses of binding profiles of all MSL components together with the comparison of profiles of other

transcription/replication factors and histone modifications will certainly help our understanding of H4-K16 acetylation and dosage compensation in *Drosophila*.

Materials and methods

ChIP

Chromatin was prepared either from overnight 0–14-h embryos or tightly staged 4–6-h embryos (after two rounds of 1-h prelay) according the protocol developed by Orlando et al. (1997). The fragments generated were 500 base pairs (bp) in average length. Chromatin from salivary glands of third instar larvae was prepared using the following procedure: Salivary glands (10 per ChIP) were fixed for 15 min at room temperature in 1 mL of fixing solution (50 mM HEPES at pH 7.6, 100 mM NaCl, 0.1 mM EDTA at pH 8, 0.5 mM EGTA at pH 8, 2% formaldehyde) on a rotating wheel. The salivary glands were then centrifuged at 2000 rpm for 1 min, washed once in PBS supplemented in 0.01% Triton X-100 and 0.125 M glycine, and then washed sequentially for 10 min each in 1 mL of 0.25% Triton X-100, 10 mM EDTA (pH 8), 0.5 mM EGTA (pH 8), and 10 mM Tris (pH 8), and in 200 mM NaCl, 10 mM Tris (pH 8), 10 mM EDTA (pH 8), and 0.5 mM EGTA (pH 8). The glands were then resuspended in 500 µL of sonication buffer (10 mM Tris at pH 8, 1 mM EDTA at pH 8, 0.5 mM EGTA at pH 8.0) and sonicated 8 min (pulsed eight times for 30 sec, paused for 30 sec, high) in a Bioruptor (Cosmo Bio). Samples were then adjusted in 0.5% sarcosyl, incubated on a wheel for 10 min at room temperature, centrifuged at 14,000 rpm for 10 min, and dialyzed overnight at 4°C against 5% glycerol, 10 mM Tris (pH 8), 1 mM EDTA (pH 8), and 0.5 mM EGTA (pH 8). The fragments generated were 500 bp on average.

Immunoprecipitation was then performed on 500 µL of chromatin from embryos or salivary glands, according to Orlando et al. (1997), using 3 µL of a polyclonal antibody against MSL-1 (kindly provided by John Lucchesi, University of Atlanta, Atlanta, GA), a polyclonal antibody against MSL-3, or a preimmune rabbit anti-serum (mock ChIP). The immunoprecipitated DNA was resuspended in 100 µL of H_2O.

DNA amplification and array hybridization for ChIP–chip experiments

DNA amplification was performed using a protocol adapted from Robyr and Grunstein (2003). Briefly, a partially degenerated oligonucleotide (5′-GTTTCCCAGTCACGATCNNNNN NNNN-3′) was first incorporated to the immunoprecipitated DNA by the following reaction: 7 µL of the immunoprecipitated DNA were incubated with 2 µL of 5× sequenase buffer (USB) and 40 pmol of the degenerated primer, heated for 2 min at 94°C, rapidly cooled to 10°C, and held for 5 min at 10°C. Five microliters of a mixture containing 1× Sequenase Buffer, 0.9 mM dNTP, 15 mM DTT, 0.75 µg BSA, and 4 U of sequenase 2.0 (USB) were then added to the reaction. The reaction was ramped to 37°C at a rate of 0.1°C/sec and then held at 37°C for 8 min. The whole process (denaturation, annealing, elongation) is repeated once, with the exception that only 4 U of the sequenase is added after the denaturation step. At the end, the samples were diluted to a final volume of 60 µL. A simple PCR was then performed on 15 µL of the samples, using the fixed sequence of the degenerated oligonucleotide (5′-GTTTCCCAGTCACG ATC-3′) and the Taq polymerase (Invitrogen). Amplified DNA was then purified on Qiagen column and eluted in 50 µL of water. Five-hundred nanograms of the amplified DNA were

then labeled using the random priming labeling kit (Invitrogen), with either 3 µL of Cy3dCTP (for the mock ChIP) or Cy5dCTP (for the MSL1 or MSL3 ChIP) (Amersham). The dNTP mixture from the random priming labeling kit was replaced by a mixture containing 1.2 mM dATP, 1.2 mM dTTP, 1.2 mM dGTP, and 0.6 mM dCTP. Five-hundred nanograms of the two probes were then mixed, purified on Qiagen column, concentrated on MicroconYM-30 (Millipore), dried, and resuspended in 2.8 µL of water. The hybridization was performed overnight at 43°C, in 40 µL of hybridization buffer (3× SSC, 50% formamide, 0.8 mg/mL polyA$^+$ [Sigma, catalog no. P9403], 1% SDS, 5× Denhardt). The slides were washed once in SDS 0.03%, 1× SSC; once in 0.2× SSC; and twice in 0.05% SSC; and centrifuged for 5 min before scanning.

RNA extraction, amplification, and array hybridization for RNA expression analysis

RNA was extract from staged dechorionated embryos or from dissected salivary glands, using the RNeasy kit (Qiagen). For the reference sample, RNA from overnight (0–12 h) embryos, adults, and salivary glands was mixed at a ratio 1:1:1. One microgram of total RNA was reverse-transcribed and amplified with 13 cycles of PCR, according to the SMART protocol described in Petalidis et al. (2003). The DNA was purified on a Qiagen column prior to labeling. Five-hundred nanograms of this amplified DNA were labeled using the Bioprime DNA Labeling System (InVitrogen) and Cy3 or Cy5-dUTP (Amersham). One microgram of each labeled cDNA was used for hybridization. The hybridization is performed on the cDNA arrays, as described above.

Array design

For hybridizations we used spotted microarrays containing *Drosophila* Gene Collection release 1 (DGCr1) (5849 clones) and release 2 (DGCr2) (5061 clones) cDNA fragments, representing >70% of the predicted genes in *Drosophila* (Berkeley *Drosophila* Genome Project; Stapleton et al. 2002). Clones were amplified by PCR directly from fresh culture. After purification, the PCR products were spotted on Corning Ultra Gaps slides using a Lucidea Array Spotter and cross-linked by applying 300 mV of UV energy.

Real-time PCR analysis

The primers pairs were designed to amplify 150–200-bp fragments in the middle of the genes, except for the *roX1* primers, designed in the previously characterized MSL-binding site.

Real-time PCR analysis of the ChIP was performed using the SYBR Green PCR master mix (Applied Biosystem), 100 ng of each primers, and 4 µL of the immunoprecipitated DNA, in an ABI7500 Real-time PCR Instrument (Applied Biosystem). Fold enrichment was determined for each primer according the Δct analysis ($2^{Ct(specific\ antibody)-Ct(mock\ antibody)}$), using three different ChIP experiments. For the analysis of the RNA levels, the RNA was first reverse-transcribed using the SuperScript RT (InVitrogen), and 500 ng of random hexamer. One microliter of cDNA was then submitted to real-time PCR using the SYBR Green PCR master mix (Applied Biosystem) and 100 ng of each primer.

Immunofluorescence on polytenes squashes

Preparation of polytene chromosomes was performed as described (http://www.igh.cnrs.fr/equip/cavalli/Lab%20Protocols/ Immunostaining.pdf). Rat MSL-1 antibody was used at 1:1000 dilution. S5-P-PolII antibody (H14) was purchased from Covance and used at a 1:50 dilution. Spt5 and Spt6 were a gift from

Dr J.T. Lis (Cornell University, NY) and both used at a 1:1000 dilution. Images were captured with an AxioCamHR CCD camera on a Zeiss Axiovert200M microscope using a 100× PlanApochomat NA 1.4 oil immersion objective. Alternatively, images were taken using appropriate filter combinations with a Deltavision Spectris optical sectioning microscope (DeltaVision).

Preprocessing, normalization and analysis

For both expression and enrichment studies, all files were processed and analyzed in the R/Bioconductor programming environment. To remove systematic sources of variation, the data were normalized using the scaled print-tip loess normalization of Yang et al. (2002) within slides and across slides. Both raw and normalized data were visually inspected for outliers and to determine if distributional assumptions were met and if normalization was appropriate. Any spots flagged during visual inspection and gridding were removed from the analysis. When log signal or fold change is reported, it represents the average across all biological replicates (minimum biological replicates was three, maximum was five; see Supplemental Material). For the ChIP–chip experiments median percentile rank was also computed across replicates. A one-sample t-test was performed to identify those clones in which enrichment was greater than mock/background (i.e., log ratio > 0). To identify the candidate MSL-1 target population, we used the joint criteria of statistical significance and rank (raw p-value < 0.1 and median percentile rank across the arrays >95%). Given the discovery framework of this study (in which false negatives would have a more detrimental impact, with respect to identification of putative candidates for further follow up, than false positives), raw p-values were used in the candidate target criteria for all subsequent analyses, instead of false discovery rate (FDR)-adjusted p-values.

For the male and female expression studies, P-values were adjusted for multiple comparisons using the Benjamini-Hochberg correction.

For analysis of categorical data, χ^2 or Fisher's exact tests were performed as appropriate. In addition to differential gene expression analysis, cluster analysis (average linkage using a correlation metric) was performed as well to aid in visualization (Cluster and Treeview software, http://rana.lbl.gov/EisenSoftware.htm).

References

Aggarwal, B.D. and Calvi, B.R. 2004. Chromatin regulates origin activity in *Drosophila* follicle cells. *Nature* **430:** 372–376.

Akhtar, A. and Becker, P.B. 2000. Activation of transcription through histone H4 acetylation by MOF, an acetyl transferase essential for dosage compensation in *Drosophila. Mol. Cell* **5:** 367–375.

Arbeitman, M.N., Furlong, E.E., Imam, F., Johnson, E., Null, B.H., Baker, B.S., Krasnow, M.A., Scott, M.P., Davis, R.W., and White, K.P. 2002. Gene expression during the life cycle of *Drosophila melanogaster. Science* **297:** 2270–2275.

Baker, B.S., Gorman, M., and Marin, I. 1994. Dosage compensation in *Drosophila. Annu. Rev. Genet.* **28:** 491–521.

Belyakin, S.N., Christophides, G.K., Alekseyenko, A.A., Kriventseva, E.V., Belyaeva, E.S., Nanayev, R.A., Makunin, I.V., Kafatos, F.C., and Zhimulev, I.F. 2005. Genomic analysis of *Drosophila* chromosome underreplication reveals a link between replication control and transcriptional territories. *Proc. Natl. Acad. Sci.* **102:** 8269–8274.

Bone, J.R., Lavender, J., Richman, R., Palmer, M.J., Turner, B.M., and Kuroda, M.I. 1994. Acetylated histone H4 on the male X chromosome is associated with dosage compensation in *Drosophila. Genes & Dev.* **8:** 96–104.

Bourbon, H.M., Gonzy-Treboul, G., Peronnet, F., Alin, M.F., Ardourel, C., Benassayag, C., Cribbs, D., Deutsch, J., Ferrer, P., Haenlin, M., et al. 2002. A P-insertion screen identifying novel X-linked essential genes in *Drosophila. Mech. Dev.* **110:** 71–83.

Bussemaker, H.J., Li, H., and Siggia, E.D. 2001. Regulatory element detection using correlation with expression. *Nat. Genet.* **27:** 167–171.

Chambeyron, S. and Bickmore, W.A. 2004. Chromatin decondensation and nuclear reorganization of the HoxB locus upon induction of transcription. *Genes & Dev.* **18:** 1119–1130.

Chiang, P.W. and Kurnit, D.M. 2003. Study of dosage compensation in *Drosophila. Genetics* **165:** 1167–1181.

Demakova, O.V., Kotlikova, I.V., Gordadze, P.R., Alekseyenko, A.A., Kuroda, M.I., and Zhimulev, I.F. 2003. The MSL complex levels are critical for its correct targeting to the chromosomes in *Drosophila melanogaster. Chromosoma* **112:** 103–115.

Dion, M.F., Altschuler, S.J., Wu, L.F., and Rando, O.J. 2005. Genomic characterization reveals a simple histone H4 acetylation code. *Proc. Natl. Acad. Sci.* **102:** 5501–5506.

Edgar, B.A. and Orr-Weaver, T.L. 2001. Endoreplication cell cycles: More for less. *Cell* **105:** 297–306.

Fagegaltier, D. and Baker, B.S. 2004. X chromosome sites autonomously recruit the dosage compensation complex in *Drosophila* males. *PLoS Biol.* **2:** e341.

Franke, A., Dernburg, A., Bashaw, G.J., and Baker, B.S. 1996. Evidence that MSL-mediated dosage compensation in *Drosophila* begins at blastoderm. *Development* **122:** 2751–2760.

Greenberg, A.J., Yanowitz, J.L., and Schedl, P. 2004. The *Drosophila* GAGA factor is required for dosage compensation in males and for the formation of the male-specific-lethal complex chromatin entry site at 12DE. *Genetics* **166:** 279–289.

Hamada, F.N., Park, P.J., Gordadze, P.R., and Kuroda, M.I. 2005. Global regulation of X chromosomal genes by the MSL complex in *Drosophila melanogaster. Genes & Dev.* **19:** 2289–2294.

Henry, R.A., Tews, B., Li, X., and Scott, M.J. 2001. Recruitment of the male-specific lethal (MSL) dosage compensation complex to an autosomally integrated roX chromatin entry site correlates with an increased expression of an adjacent reporter gene in male *Drosophila. J. Biol. Chem.* **276:** 31953–31958.

Hilfiker, A., Hilfiker-Kleiner, D., Pannuti, A., and Lucchesi, J.C. 1997. mof, a putative acetyl transferase gene related to the Tip60 and MOZ human genes and to the SAS genes of yeast, is required for dosage compensation in *Drosophila. EMBO J.* **16:** 2054–2060.

Hirose, F., Yamaguchi, M., and Matsukage, A. 1999. Targeted expression of the DNA binding domain of DRE-binding factor, a *Drosophila* transcription factor, attenuates DNA replication of the salivary gland and eye imaginal disc. *Mol.*

Cell. Biol. **19:** 6020–6028.

Hochheimer, A., Zhou, S., Zheng, S., Holmes, M.C., and Tjian, R. 2002. TRF2 associates with DREF and directs promoter-selective gene expression in *Drosophila. Nature* **420:** 439–445.

Jin, Y., Wang, Y., Johansen, J., and Johansen, K.M. 2000. JIL-1, a chromosomal kinase implicated in regulation of chromatin structure, associated with the male specific lethal (MSL) dosage compensation complex. *J. Cell Biol.* **149:** 1005–1010.

Kelley, R.L., Meller, V.H., Gordadze, P.R., Roman, G., Davis, R.L., and Kuroda, M.I. 1999. Epigenetic spreading of the *Drosophila* dosage compensation complex from *roX* RNA genes into flanking chromatin. *Cell* **98:** 513–522.

Kotlikova, I.V., Demakova, O.V., Semeshin, V.F., Shloma, V.V., Boldyreva, L.V., Kuroda, M.I., and Zhimulev, I.F. 2006. The *Drosophila* dosage compensation complex binds to polytene chromosomes independently of developmental changes in transcription. *Genetics* **172:** 963–974.

Kurdistani, S.K., Tavazoie, S., and Grunstein, M. 2004. Mapping global histone acetylation patterns to gene expression. *Cell* **117:** 721–733.

Lucchesi, J.C., Kelly, W.G., and Panning, B. 2005. Chromatin remodeling in dosage compensation. *Annu. Rev. Genet.* **39:** 615–651.

Lyman, L.M., Copps, K., Rastelli, L., Kelley, R.L., and Kuroda, M.I. 1997. *Drosophila* male-specific lethal-2 protein: Structure/function analysis and dependence on MSL-1 for chromosome association. *Genetics* **147:** 1743–1753.

MacAlpine, D.M., Rodriguez, H.K., and Bell, S.P. 2004. Coordination of replication and transcription along a *Drosophila* chromosome. *Genes & Dev.* **18:** 3094–3105.

Mendjan, S., Taipale, M., Kind, J., Holz, H., Gebhardt, P., Schelder, M., Vermeulen, M., Buscaino, A., Duncan, K., Mueller, J., et al. 2006. Nuclear pore components are involved in the transcriptional regulation of dosage compensation in *Drosophila. Mol. Cell* (in press).

Nowak, S.J. and Corces, V.G. 2004. Phosphorylation of histone H3: A balancing act between chromosome condensation and transcriptional activation. *Trends Genet.* **20:** 214–220.

Oh, H., Park, Y., and Kuroda, M.I. 2003. Local spreading of MSL complexes from *roX* genes on the *Drosophila* X chromosome. *Genes & Dev.* **17:** 1334–1339.

Orlando, V., Strutt, H., and Paro, R. 1997. Analysis of chromatin structure by in vivo formaldehyde cross-linking. *Methods* **11:** 205–214.

Park, Y., Kelley, R.L., Oh, H., Kuroda, M.I., and Meller, V.H. 2002. Extent of chromatin spreading determined by roX RNA recruitment of MSL proteins. *Science* **298:** 1620–1623.

Petalidis, L., Bhattacharyya, S., Morris, G.A., Collins, V.P., Freeman, T.C., and Lyons, P.A. 2003. Global amplification of mRNA by template-switching PCR: Linearity and application to microarray analysis. *Nucleic Acids Res.* **31:** e142.

Peter, A., Schottler, P., Werner, M., Beinert, N., Dowe, G., Burkert, P., Mourkioti, F., Dentzer, L., He, Y., Deak, P., et al. 2002. Mapping and identification of essential gene functions on the X chromosome of *Drosophila. EMBO Rep.* **3:** 34–38.

Ragoczy, T., Telling, A., Sawado, T., Groudine, M., and Kosak, S.T. 2003. A genetic analysis of chromosome territory looping: Diverse roles for distal regulatory elements. *Chromosome Res.* **11:** 513–525.

Rastelli, L., Richman, R., and Kuroda, M.I. 1995. The dosage compensation regulators MLE, MSL-1 and MSL-2 are interdependent since early embryogenesis in *Drosophila. Mech. Dev.* **53:** 223–233.

Robyr, D. and Grunstein, M. 2003. Genomewide histone acety-

lation microarrays. *Methods* **31:** 83–89.

Sass, G.L., Pannuti, A., and Lucchesi, J.C. 2003. Male-specific lethal complex of *Drosophila* targets activated regions of the X chromosome for chromatin remodeling. *Proc. Natl. Acad. Sci.* **100:** 8287–8291.

Schubeler, D., Francastel, C., Cimbora, D.M., Reik, A., Martin, D.I., and Groudine, M. 2000. Nuclear localization and histone acetylation: A pathway for chromatin opening and transcriptional activation of the human β-globin locus. *Genes & Dev.* **14:** 940–950.

Schubeler, D., Scalzo, D., Kooperberg, C., van Steensel, B., Delrow, J., and Groudine, M. 2002. Genome-wide DNA replication profile for *Drosophila melanogaster*: A link between transcription and replication timing. *Nat. Genet.* **32:** 438–442.

Smith, E.R., Allis, C.D., and Lucchesi, J.C. 2001. Linking global histone acetylation to the transcription enhancement of X-chromosomal genes in *Drosophila* males. *J. Biol. Chem.* **276:** 31483–31486.

Stapleton, M., Liao, G., Brokstein, P., Hong, L., Carninci, P., Shiraki, T., Hayashizaki, Y., Champe, M., Pacleb, J., Wan, K., et al. 2002. The *Drosophila* gene collection: Identification of putative full-length cDNAs for 70% of *D. melanogaster* genes. *Genome Res.* **12:** 1294–1300.

Straub, T., Dahlsveen, I.K., and Becker, P.B. 2005a. Dosage compensation in flies: Mechanism, models, mystery. *FEBS Lett.* **579:** 3258–3263.

Straub, T., Gilfillan, G.D., Maier, V.K., and Becker, P.B. 2005b. The *Drosophila* MSL complex activates the transcription of target genes. *Genes & Dev.* **19:** 2284–2288.

Taipale, M. and Akhtar, A. 2005. Chromatin mechanisms in *Drosophila* dosage compensation. *Prog. Mol. Subcell. Biol.* **38:** 123–149.

Turner, B.M. 1998. Histone acetylation as an epigenetic determinant of long-term transcriptional competence. *Cell. Mol. Life Sci.* **54:** 21–31.

Turner, B.M., Birley, A.J., and Lavender, J. 1992. Histone H4 isoforms acetylated at specific lysine residues define individual chromosomes and chromatin domains in *Drosophila* polytene nuclei. *Cell* **69:** 375–384.

van Steensel, B. 2005. Mapping of genetic and epigenetic regulatory networks using microarrays. *Nat. Genet.* **37 (Suppl.):** S18–S24.

Wang, Y., Zhang, W., Jin, Y., Johansen, J., and Johansen, K.M. 2001. The Jil-1 tandem kinase mediates histone H3 phosphorylation and is required for maintenance of chromatin structure in *Drosophila. Cell* **105:** 433–443.

White, E.J., Emanuelsson, O., Scalzo, D., Royce, T., Kosak, S., Oakeley, E.J., Weissman, S., Gerstein, M., Groudine, M., Snyder, M., et al. 2004. DNA replication-timing analysis of human chromosome 22 at high resolution and different developmental states. *Proc. Natl. Acad. Sci.* **101:** 17771–17776.

Yang, Y.H., Dudoit, S., Luu, P., Lin, D.M., Peng, V., Ngai, J., and Speed, T.P. 2002. Normalization for cDNA microarray data: A robust composite method addressing single and multiple slide systematic variation. *Nucleic Acids Res.* **30:** e15.